Improved HCF Performance and FOD Tolerance of Surface Treated Ti-6-2-4-6 Compressor Blades

Paul S. Prevéy
Director of Research, Lambda Research,
Cincinnati, OH 45227-3401
N. Jayaraman
Director of Materials Research, Lambda Research, Cincinnati, OH 45227-3401
Michael J. Shepard
Air Force Research Laboratory, Materials and Manufacturing Directorate, AFRL/MLLMN,
WPAFB, OH, 45433-7817

ABSTRACT

High cycle fatigue (HCF) strength and the resistance to foreign object damage (FOD) can be improved by the use of mechanical surface treatments like shot peening and low plasticity burnishing (LPB) to introduce beneficial surface layers of compressive residual stress. In this paper, results from an extensive study of the relative effects of these two surface treatments on the residual stress, cold work distributions, HCF performance, and FOD tolerance of alloy Ti-6Al-2Sn-4Zr-6Mo (Ti-6-2-4-6) are presented. The compressive layer produced by LPB is shown to be stable even after thermal exposure to 371C. Blade-edge bending fatigue specimens were designed to simulate the leading edge of an integral bladed rotor (IBR) compressor blade. FOD was simulated by controlled size notches introduced on the specimens using electrical discharge machining (EDM). Both disk and blade simulation specimens with 0.5 mm (0.020 in) deep FOD had HCF strengths after LPB over 4-times higher than 8A shot peening. The HCF performance after LPB was relatively unaffected by FOD up to 0.75 mm (0.030 in) deep. FOD up to 2.5 mm (0.10 in) in depth after LPB decreased the fatigue strength only nominally. If the traditional design criterion of Kt (notch sensitivity factor) of 3 were to be used, LPB effectively mitigated FOD damage up to 2.5 mm (0.10 in) deep.

INTRODUCTION

HCF accounts for 56% of major aircraft engine failures[1], and ultimately limits the service life of most critical rotating components. Many engine components are prone to HCF failure because of high mean operating stresses and temperatures in the high-pressure stages, and FOD in the low-pressure stages. FOD creates crack initiation sites and reduces the HCF strength by at least half. Because ingestion of HCF failed components can cause catastrophic engine failure, extensive inspection and maintenance programs are required to detect and replace damaged parts. An estimated $400M[1] is expended annually for HCF related inspection and maintenance, greatly increasing the total ownership cost of military aircraft. As the fleet continues to age, the costs for engine inspection and maintenance are projected to increase exponentially. The associated reduction in time on-wing increasingly impacts fleet readiness. A new approach and new technology are needed that will reduce, or even arrest, the spiraling costs of HCF mitigation.

Surface residual compressive stresses in metallic components have long been recognized[2-5] to lead to enhanced fatigue strength. For example, many engineering components have been shot-peened or cold worked with fatigue strength enhancement as the primary objective. Other examples of surface treatments like LPB,[6] laser shock peening (LSP),[7] and ultrasonic peening have emerged. These different surface treatment methods have been shown to benefit fatigue prone engineering components to different degrees. LPB has been demonstrated to be a practical surface treatment method providing a deep surface layer of high magnitude compression in various aluminum, titanium, nickel based alloys and steels. Unlike other surface treatment methods, the cold work associate with this treatment is usually limited to < 5% cold work. The lower cold work results in very stable residual stresses even under mechanical overload and elevated temperature conditions. The deep stable compressive residual stress state on the surface of these materials has been shown to be effective in mitigating damage due to FOD,[8] fretting fatigue,[9] corrosion fatigue[10], and stress corrosion cracking.[11] This surface treatment process can be performed on conventional CNC machine tools at costs and speeds comparable to conventional machining operations such as surface milling. By improving damage tolerance

9th National Turbine Engine High Cycle Fatigue Conference
Pinehurst, North Carolina
March 16-19, 2004

and HCF strength of critical engine components, LPB provides an affordable means of both improving engine life and reducing ownership costs.

The objective of this research was to demonstrate the feasibility of improving HCF life and damage tolerance using LPB surface treatment to create zones of high compressive residual stress in areas prone to FOD and fatigue crack initiation in the alloy Ti-6-2-4-6 used for making a 4th stage IBR. Surface treatment parameters were developed for specimens designed to simulate blade edge and thick section conditions to achieve through-thickness compression in blade edge specimens and deep surface compression in plate specimens using existing tools. Current practice requires the replacement of blades containing detectable FOD as small as 0.127 mm (0.005 in) in the 4th stage IBR. This effort proved that appropriate surface treatment increases the allowable FOD to over 0.762 mm (0.030 in).

METHODS

Material and Processing

TI-6-2-4-6 material (beta-forged and heat treated) was received in the shape of a portion of the forging for an IBR. Slightly less than half the forging was received. A total of 7 beam specimens, 48 thick section four-point bend bar and 44 blade-edge feature specimens were prepared from this forging. Chemistry and tensile properties of the material were verified, as follows.

The chemistry (wt %) by spectroscopic analysis:

Analysis:	Ti – 81.6%	Al – 5.79%Mo – 6.74% Sn – 1.94% Zr – 3.89%
Nominal:	Ti – Balance	Al – 5.5-6.5Mo – 5.5-6.5 Sn – 1.8-2.2 Zr – 3.6-4.4

The tensile properties compared to TIMET data sheets for the beta-forged condition and the actual tensile properties measured for the material are as follows:

	YS (ksi)	UTS (ksi)	% elong.	% RA
TI-6-2-4-6	146.8	168.3	7.8	20.1
TIMET data	152	174	6.5	13

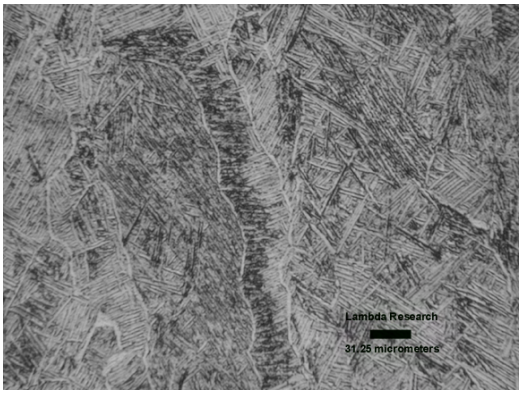

(a)

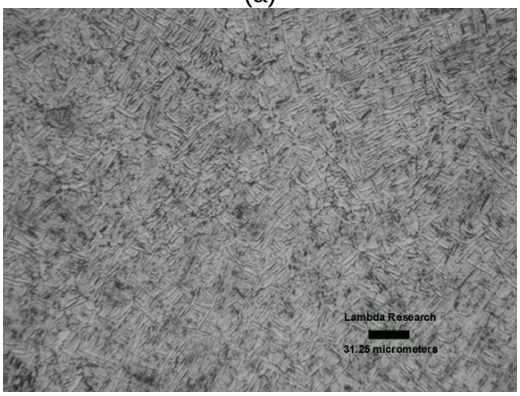

(b)

Figure 1: Photomicrographs showing the Widmanstatten structure of the TI-6-2-4-6 material, (a) Axial, looking into the bore, (b) Radial, looking down on the disk.

The material exhibited a Widmanstatten structure as shown in the photomicrographs taken in different orientations in Figures 1a and b.

Specimen and FOD Design

Thick section and blade edge specimens (Figures 2a and b) were designed for determination of surface treatment parameters and HCF testing. The thick section specimen with a trapezoidal cross section in the gage was designed to test the effectiveness of surface treatments under HCF conditions. The trapezoidal cross section, when tested under 4-point bending fatigue conditions, limits the maximum applied tensile stress to be on the treated top surface. The blade-edge simulation specimens were designed to specifically simulate the geometrical conditions of the leading edge of the 4th stage IBR blades.

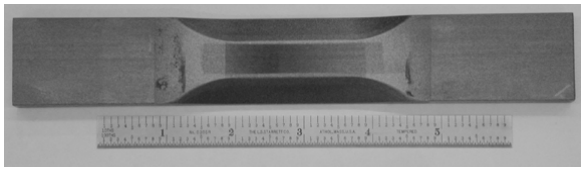

(a)

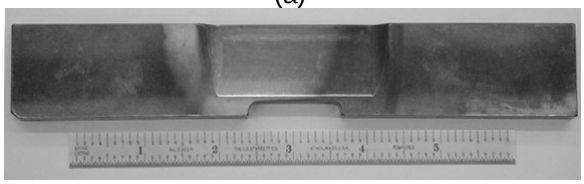

(b)

Figure 2: Photographs of LPB processed (a) thick section specimen, and (b) blade-edge specimen.

Fatigue tests were performed on specimens with simulated FOD in the form of a nominal semi-elliptical electrical discharge machined (EDM) flaw with a depth, a = 0.254 mm (0.010 in) and surface length, 2c = 1.524 mm (0.060 in) FOD was introduced after the surface treatment procedure, but before exposure to the engine operating temperature, to simulate damage occurring prior to, or during, engine service. Figures 3a and b show the shape and size of typical EDM simulated FOD in a thick section specimen (on a machined surface). Figures 4a and b show the shape and size of typical EDM simulated FOD in a blade edge feature specimen. FOD was introduced into the "leading edge" of the blade-edge fatigue samples as a narrow 0.254mm (0.010 in) wide EDM slot cut entirely across the edge of the blade at the center of the gage section. The form of the EDM notches produced was essentially a flat-bottomed rectangular slot with a highly tensile and cracked EDM recast layer exposed at the bottom surface of the notch.

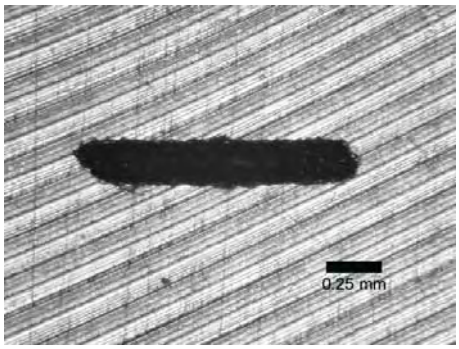

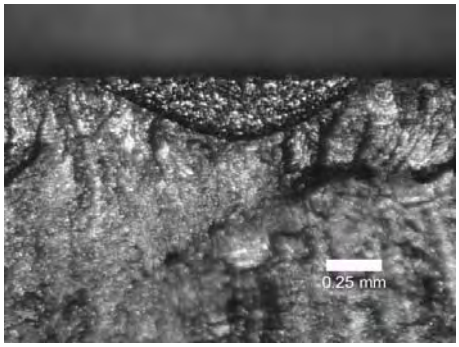

Figure 3: Optical photomicrographs showing (a) the top surface of a typical thick section specimen (as-milled surface condition) with the FOD of ao = 0.254 mm (0.010 in) and 2co = 1.524 mm (0.060 in) (b) fracture surface of a typical thick section specimen with the same FOD. The re-cast layer is evident as shiny speckles in the FOD area.

Low Plasticity Burnishing

The LPB process has been described in detail previously[6,8] and is characterized by a single pass of a smooth free rolling ball under a normal force sufficient to plastically deform the surface of the material. Hertzian loading creates a layer of compressive residual stress, the depth of which depends on process parameters. The ball is supported in a fluid bearing with sufficient pressure to lift it off the surface of the retaining spherical socket. The ball is in solid contact only with the surface to be burnished, and is free to roll on the surface of the work piece, eliminating shear deformation and tool drag.

Using CNC positioning, the tool path is controlled so that the surface is covered with a series of passes at a separation maintained to achieve maximum compression with minimum cold working. The tool may be moved in any direction along the surface of a complex work piece, as in a typical multi-axis CNC machining operation.

Processing of fatigue specimens (both thick section and blade-edge type) used in this investigation is depicted in Figures 5a and b. Using caliper tooling to simultaneously burnish both sides of the blade edge specimen, a region of nominally 12.7 mm (0.5 in) (chord wise) throughout the gauge section of the blade-edge specimen was burnished using a 4-axis CNC facility built around a conventional 20 hp machining center.

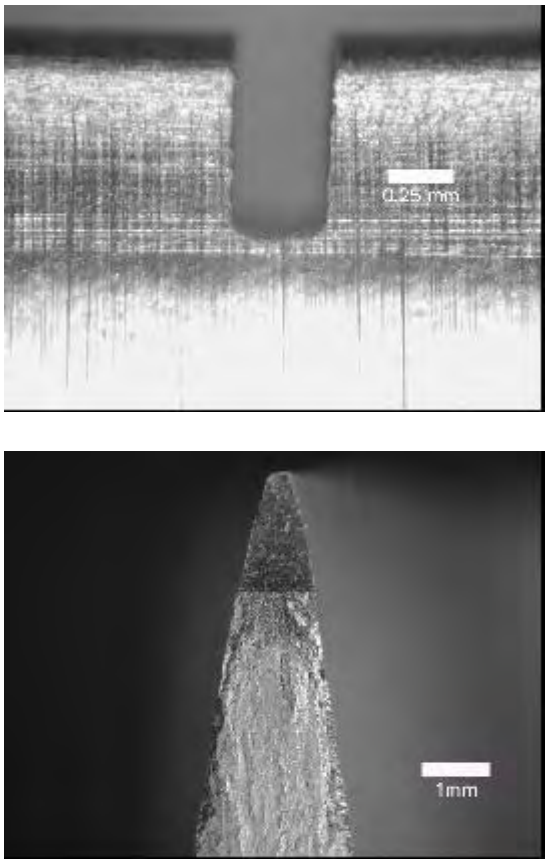

Figure 4: Optical photomicrographs showing (a) the side face of a typical blade edge specimen with the FOD of ao = 0.762 mm (0.030 in) (b) the fracture surface of a typical blade edge specimen with the FOD of ao = 1.905 mm (0.075 in) Note the simulated blade-edge is designed to closely simulate the geometric (angle and radius) conditions of the blade edge.

Surface Characterization

Residual stress and cold work measurements were made by the standard x-ray diffraction $\sin^2\psi$ technique[12,13] on the surface and at several depths below the surface after successively electropolishing on LPB treated and SP specimens.

Surface roughness values were obtained using a Mitutoyo SJ-201 Surface Roughness Tester. The Ra surface roughness, defined as the arithmetic mean of the absolute values of the profile deviations from the mean line, was calculated both perpendicular to the specimen axis and parallel to the specimen axis.

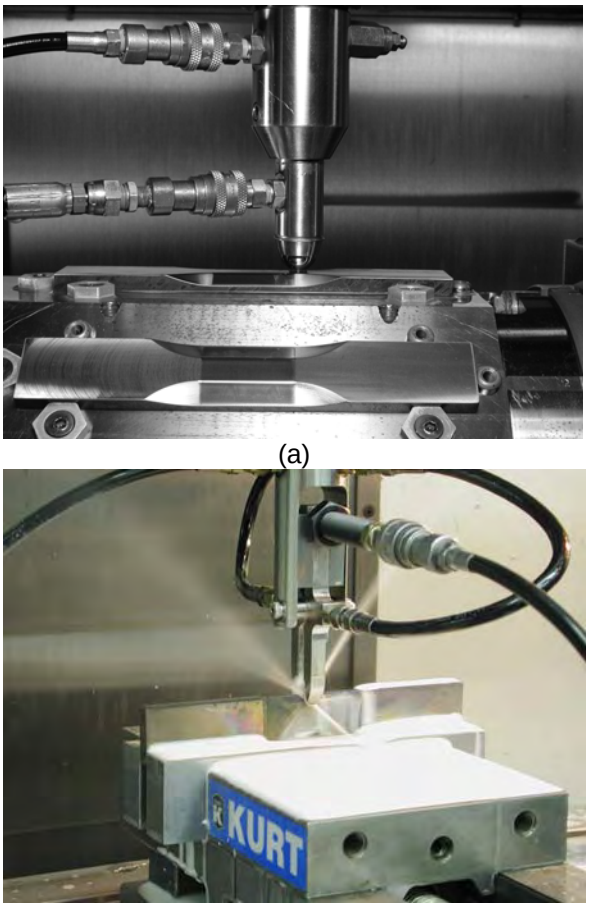

(a)

(b)

Figure 5: LPB processing in a 4-axis CNC mill – (a) thick section fatigue samples with a single point contact tool. (b) blade-edge fatigue sample with a caliper style tool.

High Cycle Fatigue Testing

All high cycle fatigue tests were performed under constant stress amplitude load at ambient temperature in four-point bending on a Sonntag SF-1U fatigue machine. The cyclic frequency and load ratio, R, were 30 Hz and 0.1, respectively. Tests were conducted to specimen fracture or until a "run-out" life of 2.5×10^6 was attained, whichever occurred first.

All specimens were subjected to a temperature of 371C for 100 hours, prior to introducing the

EDM notch, to simulate FOD occurring during engine service. In the case of thick section specimens, attempts were made to run HCF tests at different stresses to failure, and generate full S-N curves. Only one EDM simulated FOD condition of 0.010 in depth was tested. In the case of blade edge feature specimens, five different EDM simulated FOD conditions were tested, with depths of 0.508, 0.716, 1.270, 1.905 and 2.540 mm (.020, .030, .050, .075 and .100 in respectively.) Due to limited samples, a step loading fatigue testing technique was used to determine the endurance limit for each FOD depth.

Following fatigue testing, each specimen was examined optically at magnifications up to 60X to identify fatigue origins and locations thereof relative to the specimen geometry. Fractographs were taken with a Nikon 990 digital camera through a Nikon SMZ-10 Stereoscope. Selected specimens were also examined using a Cambridge Stereoscan S90B SEM.

Fatigue Modeling

Fatigue life-prediction modeling analysis was performed using linear elastic fracture mechanics (LEFM) based codes developed at Lambda Research. Initial FOD sizes were used for starting crack sizes. The LEFM models are also capable of accounting for the residual stress distributions achieved by the different surface treatment methods. Since fatigue crack growth (FCG) property data were not available in the published literature for Ti-6-2-4-6, titanium alloy Ti-811 was considered to have similar crack growth behavior, and the corresponding FCG properties were used in this analysis. The residual stress profiles actually measured in TI-6-2-4-6 alloy in the SP and LPB processed conditions, shown in Figure 7, were used in the fatigue life predictions.

RESULTS AND DISCUSSION

Residual Stresses and Thermal Stability

Surface treatment parameters were developed based upon prior experience with Ti alloys. Coupons were prepared for evaluation of the residual stress and cold work distributions and compared to conventional shot peening. Subsurface residual stress and cold work distributions are shown in Figure 6. LPB provides a depth of compression nominally 7 times deeper than that of shot peening. Maximum compression achieved is nominally –827.4 MPa (–120 ksi) at a depth of 0.0254 mm (0.001 in) for shot peening and –723.9 MPa (–105 ksi) at a depth of 0.254 mm (0.010 in) for LPB. Cold work approaches 25% at the SP surface and is nominally 3% for the LPB surface.

To be effective, the layer of surface compression must be retained in engine service. Residual stress depth profiles were obtained after exposure to the maximum engine operating temperature of 371C for 100 hrs. Figure 6 shows the effect of such long exposure. The LPB processed specimen shows only minor reduction, if any, in compression following thermal exposure. As has been observed with Ti-6-4 and IN718, the surface compression for the shot peened and LSG specimens relaxed nominally 50% during thermal exposure.

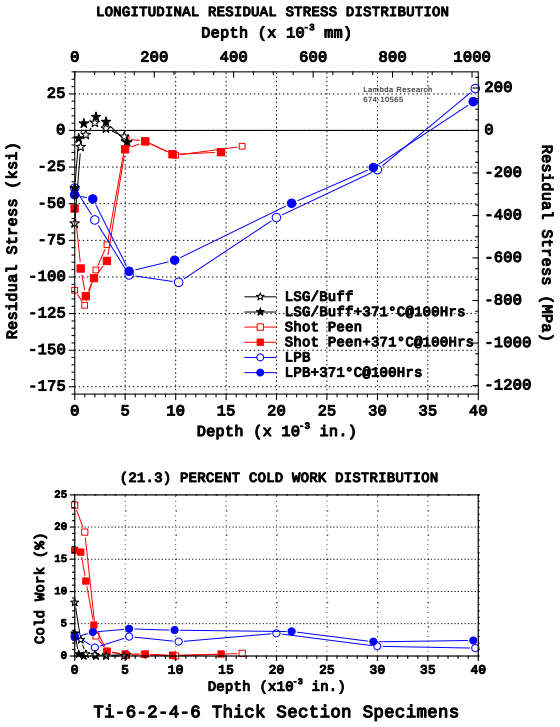

Figure 6: Subsurface residual stress and cold work distributions produced in flat plate specimens before and after thermal exposure.

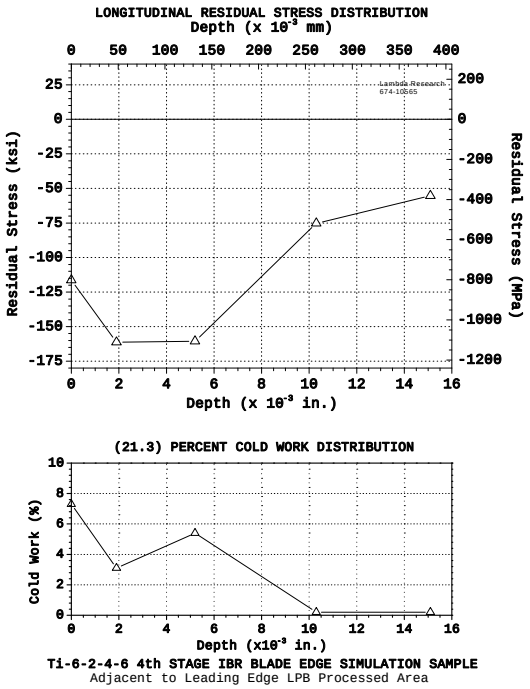

Figure 7: Residual stress distribution in the LPB blade edge specimen to nominally mid-thickness.

The though-thickness residual stress and cold work distributions produced using LPB parameters chosen for the blade-edge fatigue specimens are shown in Figure 7. The residual stresses were measured in the longitudinal (span-wise) direction adjacent to the leading edge. Measurements were made at the surface and at nominal depths up to 0.381 mm (0.015 in) the nominal mid-thickness of the blade edge. Maximum compression approaching –160 ksi occurred between depths of 0.0508 and 0.127 mm (0.002 and 0.005 in) Compression of at least –344.75 MPa (–50 ksi) was achieved to the nominal mid-thickness depth of 0.381 mm (0.015 in) indicating through-thickness compression.

Surface Roughness

Surface roughness measured for LPB, low stress ground (LSG), and shot peened (SP) surfaces are shown in Figures 8 (a) and (b). A representative bar chart of the average surface roughness for LPB, SP, and LSG surfaces of both HCF thick section and blade-edge specimens are shown in Figures 8 (a) and (b). The surface roughness was less than 0.127 μm (5 μin) for the LPB processed samples parallel to the specimen axis. The LSG samples had surface roughness values in the 0.381 to 0.508 μm (15 to 20 μin) range. The roughest surface, ranging from 2.032 to 2.54 μm (80 to 100 μin) was produced by the shot peening operation.

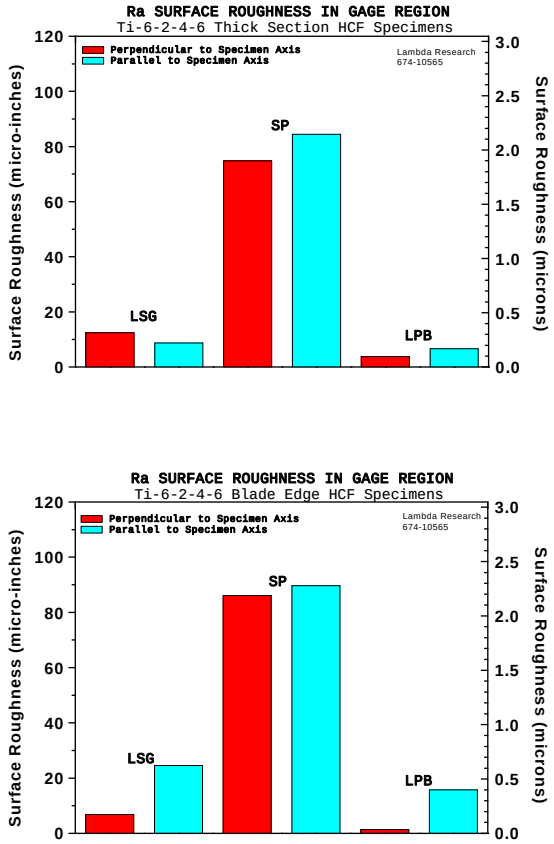

Figure 8: Bar charts showing the relative surface roughness of the gauge sections of (a) thick section and (b) blade-edge specimens in the LSG, shot peened and LPB conditions.

HCF Performance

The HCF results and the predicted S-N curves for 0.254 mm (0.010 in) deep EDM FOD in the test surface of the thick section fatigue samples are presented in Figure 9. The HCF endurance limits (for a fatigue life of 10^7 cycles) for the LSG condition and for shot peening without FOD are virtually identical, on the order of 690 to 720 MPa (100 to 105 ksi). LPB without FOD provides a slight improvement to 758 MPa (110 ksi). FOD 0.25 mm (0.010 in) deep reduces the endurance limit for the base-line material to less than 172 MPa (25 ksi). Shot peening provides virtually no benefit for 0.25 mm (0.010 in) FOD, with an endurance limit around 206 to 241 MPa (30 to 35 ksi). With prior LPB, FOD 0.25 mm (0.010 in) deep reduces the endurance limit from 758 MPa

(110 ksi) to 690 MPa (100 ksi). The thick section sample test data show that LPB provided a 3X increase in endurance limit over shot peening and complete mitigation of the fatigue debit caused by 0.25 mm (0.010 in) FOD.

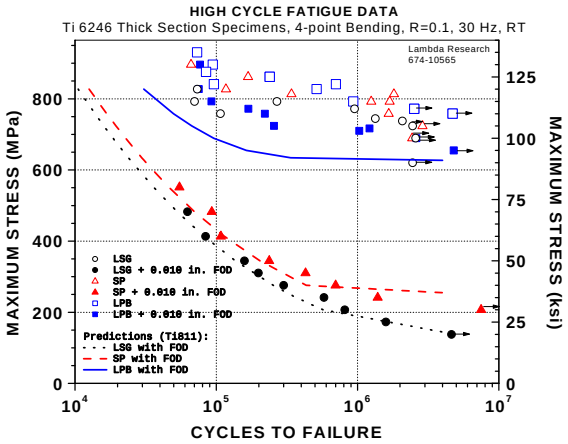

Figure 9: Thick section HCF data (S-N curve) for Ti-alloy TI-6-2-4-6 with surface treatments LSG, SP and LPB. Predictions from LEFM based models are also included. It is evident that while surface treatments had a marginal effect on HCF performance of virgin specimens, upon introduction of even small FOD, both the as-machined and SP conditions showed a dramatic loss of HCF performance, while the LPB condition showed little or no loss of HCF performance.

The fatigue lives predicted using a LEFM based approach for crack growth through the actual measured residual stress profiles confirm the empirical findings. The calculated endurance limit for the LSG condition with a 0.25 mm (0.010 in) deep FOD (no residual stress assumed) was 145 MPa (21 ksi). Shot peening is predicted to raise the endurance limit to 255 MPa (37 ksi) Both predictions are in good agreement with the fatigue results. The predicted endurance limit for the LPB processed condition is 627 MPa (91 ksi) an improvement factor of nearly 4.5 over the as-received condition. The actual endurance limit for LPB processed condition, based upon run-outs during testing, is nominally 655 MPa (95 ksi). Most of the LPB fatigue lives exceed the prediction, which may be due to the use of Ti-811 crack growth data.

Determination of the Maximum Practical FOD Tolerance for the IBR Blade Geometry

Results from the step loading high cycle fatigue tests are shown in Figure 10. Failed samples are plotted in the customary S-N curve fashion. SP samples were tested at the minimum and maximum FOD depths of 0.50 and 2.5 mm (0.020 and 0.100 in) respectively. The endurance limits, either with or without shot peening, were reduced from 620 MPa (90 ksi) to nominally 152 MPa (22 ksi) by 0.50 mm (0.020 in) deep FOD. The maximum FOD depth of 2.5 mm (0.100 in) reduced both the SP and base-line (untreated) endurance limits to nominally 103 MPa (15 ksi). LPB provided essentially complete mitigation of 0.50 and 0.72 mm (0.020 and 0.030 in) deep FOD. Larger FOD resulted in lower fatigue strength, but the deep compression produced by LPB resisted crack propagation providing an endurance limit in excess of 276 MPa (40 ksi) for even 2.5 mm (0.1 in) FOD.

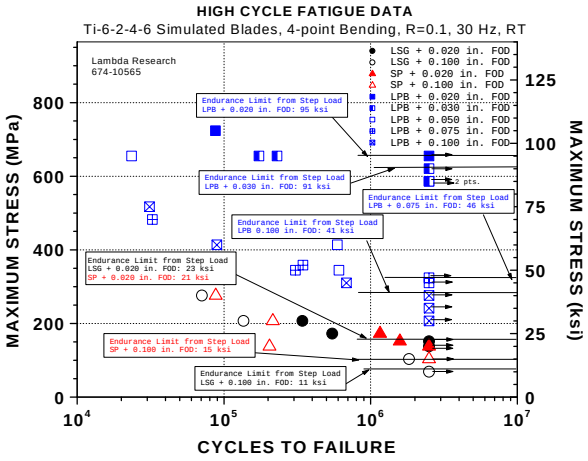

Figure 10: HCF results for Ti-alloy TI-6-2-4-6blade edge specimens–. Both S-N data and step-loading data to identify the endurance limits are presented.

The endurance limits for the range of FOD depths are summarized in Figure 11, the benefits of the compressive residual stress produced by LPB are evident in this figure. Both the baseline and the SP specimens showed very low fatigue strength around 152 MPa (22 ksi) even for FOD of 0.50 mm (0.020 in). This fatigue strength decreased marginally to 124 and 117 MPa (18 and 17 ksi) respectively, when the FOD depth increased from 0.50 to 2.5 mm (0.020 to 0.100 in).

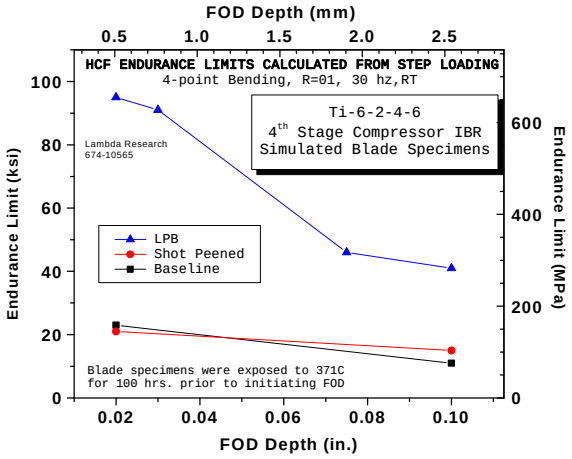

Figure 11: Effect of FOD size on the fatigue strength (10^7 cycle endurance limit) of blade-edge specimens.

In stark contrast, the LPB treated specimens showed fatigue strengths of nominally 655 MPa (95 ksi) for a FOD size of 0.50 mm (0.020 in) – nearly a factor of 5 higher than the LSG and SP specimens. For 0.72 mm (0.030 in) deep FOD, the LPB fatigue strength decreased only marginally to about 620 MPa (90 ksi) and even for FOD as deep as 2.5 mm (0.100 in) the fatigue strength remained at 276 MPa (40 ksi) nearly double the fatigue strength of the baseline and SP specimens with only a 0.50 mm (0.020 in) FOD. Given that rotating engine components are generally designed for a K_t of 3.0, the component would be expected to survive even a 2.5 mm (0.100 in) deep FOD event. These results clearly indicate the success of LPB treatment in mitigating FOD damage in Ti-alloy TI-6-2-4-6.

Generally, fractography for both the thick section and blade edge featured specimens are consistent with the fatigue results. Figures 12 and 13 show typical optical fractographs showing brittle flat fracture surfaces. Video of the LPB crack initiation and propagation showed evidence of crack initiation from the root of the notch and propagation of tunneling of cracks growing to the LPB surface.

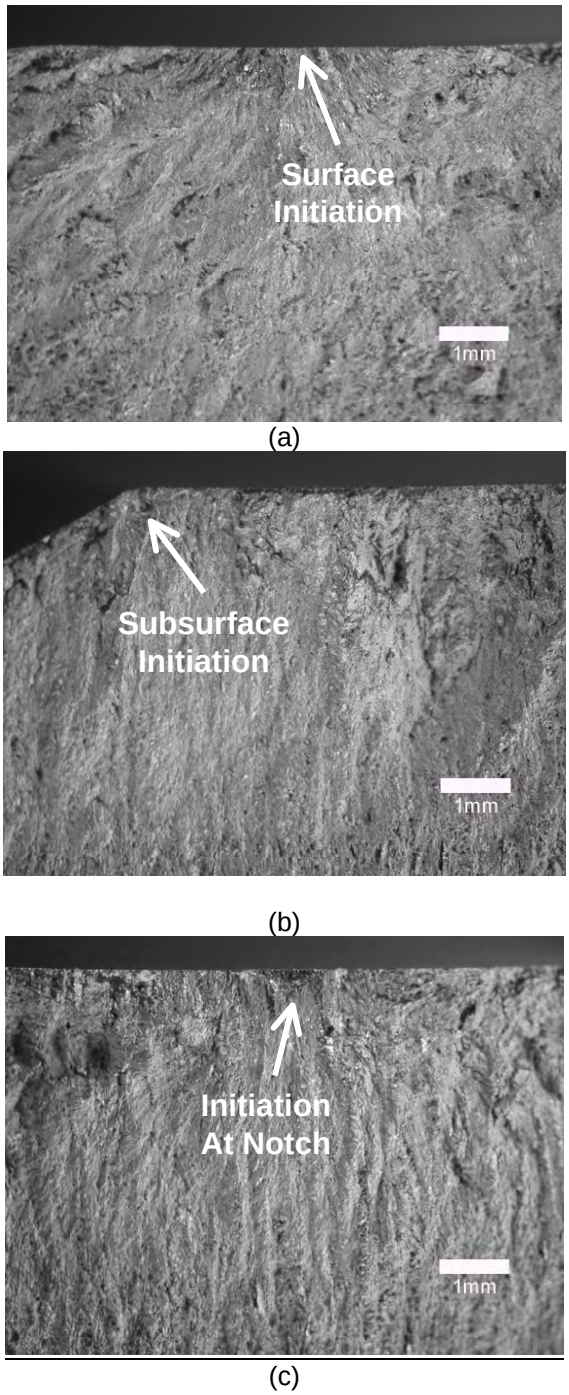

Figure 12: Typical optical fractographs for thick section specimens – (a) LPB + Thermal Exposure, Max. Stress : 130 ksi, Nf = 94,532 cycles, (b) SP + Thermal Exposure, Max. Stress : 115 ksi, Nf = 1,251,483 cycles), (c) LPB + Thermal Exposure+ 0.010 in FOD, Max. Stress : 120 ksi, Nf = 75,204 cycles)

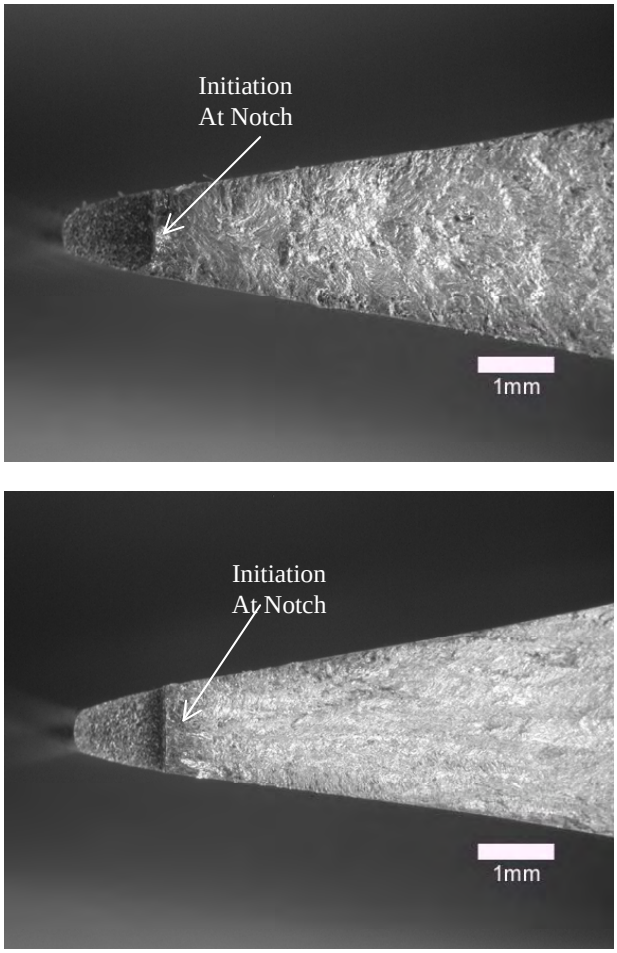

Figure 13: Typical optical fractographs for blade edge feature specimens – (a) LPB + Thermal Exposure + 0.050 in FOD, Max. Stress : 50 ksi, Nf = 609,295 cycles, (b) LPB + Thermal Exposure + 0.050 in FOD, Max. Stress : 60 ksi, Nf = 594,080 cycles

SUMMARY AND CONCLUSIONS

Low plasticity burnishing has been successfully applied to develop a region of high compressive residual stresses in TI-6-2-4-6 used for making a 4th stage IBR. A thick section specimen with a center surface semi elliptical flaw was designed to simulate the thick root section and a blade-edge feature specimen was designed to simulate the leading edge of the blade section of the IBR. LPB surface treatment resulted in a compressive layer to a depth of 0. 9 mm (0.035 in) in the thick specimens. In blade edge specimens, through-thickness compression on the order of –1100 MPa (–160 ksi) was achieved.

The endurance limit of the thick section specimens without FOD was nominally 724 MPa (105 ksi.) FOD 0.254 mm (0.010 in) deep drastically reduced the endurance limit to nominally 138 MPa (20 ksi.) The endurance limit of the SP specimens show a similar trend resulting in a drastic reduction to a nominal strength of about 240 MPa (35 ksi.)

LPB produced an endurance limit of 690 MPa (100 ksi,) which is only slightly less than that of the specimens treated with LPB without FOD. More importantly, the endurance limit of surface treated specimens with FOD was almost equal to the untreated and SP specimens without FOD.

Blade edge specimens with 0.5 mm (0.020 in) deep FOD had an endurance limit of nominally 138 MPa (20 ksi). FOD 2.5 mm (0.100 in) deep further reduced the fatigue strength slightly. At stresses above the endurance limit, the life of the blades with FOD was less than 10% of the life of an undamaged blade. Shot peening the blade edge specimens did not result in any significant improvement in fatigue strength.

Application of LPB prior to 0.50 mm (0.020 in) or 0.72 mm (0.030 in) deep FOD resulted in virtually identical fatigue strengths , with a nominal value of about 655 MPa (95 ksi.) For larger FOD sizes up to 2.5 mm (0.100 in) the fatigue strength dropped to a nominal value of about 276 MPa (40 ksi.) This is well above the 1378 MPa (20 ksi) strength achieved in the baseline specimens with only 0.50 mm (0.020 in) FOD. This improved performance of LPB treated specimens are attributed to the –1100 MPa (-160 ksi) compression achieved in blade edge specimens.

LPB has been successfully demonstrated to provide an order of magnitude improvement in the damage tolerance of TI-6-2-4-6 used in making the F119 4th stage IBR. Complete mitigation of 0.72 mm (0.030 in) FOD was achieved. Acceptable performance, indicating survival of the blade for the K_t=3 design criteria, was achieved for FOD up to 2.5 mm (0.100 in) deep. The potential now exists for significantly reducing the costs of engine inspection, maintenance, and ownership while improving engine performance and fleet readiness.

REFERENCES

1. Propulsion Directorate, AFRL/WPAFB (2000), High Cycle Fatigue (HCF) Program 1999 Annual Report, AFRL-PR-WP-TR-2000-2004.
2. N.E. Frost, K.J. Marsh, L.P. Pook, *Metal Fatigue*, Oxford University Press, 1974.
3. H.O. Fuchs, and R.I. Stephens, *Metal Fatigue In Engineerin*g, John Wiley & Sons, 1980.
4. H. Berns, and L. Weber, "Influence of Residual Stresses on Crack Growth," Impact Surface Treatment, edited by S.A. Meguid, Elsevier, 33-44, 1984.
5. J.A.M. Ferreira, L.F.P. Boorrego, and J.D.M. Costa, "Effects of Surface Treatments on the Fatigue of Notched Bend Specimens," Fatigue, Fract. Engng. Mater., Struct., Vol. 19 No.1, pp 111-117,1996.
6. P.S. Prevéy, J. Telesman, T. Gabb, and P. Kantzos, “FOD Resistance and Fatigue Crack Arrest in Low Plasticity Burnished IN718”, Proceedings of the 5th National High Cycle Fatigue Conference, Chandler, AZ. March 7-9, 2000.
7. A.H. Clauer, "Laser Shock Peening for Fatigue Resistance," Surface Performance of Titanium, J.K. Gregory, et al, Editors, TMS Warrendale, PA (1996), pp 217-230.
8. P. Prevéy, N. Jayaraman, R. Ravindranath, “Effect of Surface Treatments on HCF Performance and FOD Tolerance of a Ti-6Al-4V Vane,” Proceedings 8th National Turbine Engine HCF Conference, Monterey, CA, April 14-16, 2003
9. M. Shepard, P. Prevéy, N. Jayaraman, “Effect of Surface Treatments on Fretting Fatigue Performance of Ti-6Al-4V,” submitted to International Journal of Fatigue
10. P.S. Prevéy and J.T. Cammett, “The Influence of Surface Enhancement by Low Plasticity Burnishing on the Corrosion Fatigue Performance of AA7075-T6,” to appear in International Journal of Fatigue
11. N. Ontko and J. Coate, “Mitigation of Stress Corrosion Cracking by LPB Treatment in 300M Landing Gear Steel”, unpublished research, AFRL, December 2003.
12. M.E. Hilley, ed., (2003), Residual Stress Measurement by X-Ray Diffraction, HS *J784*, (Warrendale, PA: Society of Auto. Eng.)
13. P.S. Prevéy, (1986), “X-Ray Diffraction Residual Stress Techniques,” *Metals Handbook*, **10**, (Metals Park, OH: ASM), pp 380-392.